Cross talk in the Lambert-Beer calculation for near-infrared wavelengths estimated by Monte Carlo simulations

K. Uludag
M. Kohl
J. Steinbrink
H. Obrig
A. Villringer
Humboldt University
Department of Neurology, Charité Hospital
Schumannstrasse 20/21
10117 Berlin, Germany

Abstract. Using the modified Lambert-Beer law to analyze attenuation changes measured noninvasively during functional activation of the brain might result in an insufficient separation of chromophore changes ("cross talk") due to the wavelength dependence of the partial pathlength of photons in the activated volume of the head. The partial pathlength was estimated by performing Monte Carlo simulations on layered head models. When assuming cortical activation (e.g., in the depth of 8–12 mm), we determine negligible cross talk when considering changes in oxygenated and deoxygenated hemoglobin. But additionally taking changes in the redox state of cytochrome-c-oxidase into account, this analysis results in significant artifacts. An analysis developed for changes in mean time of flight—instead of changes in attenuation—reduces the cross talk for the layers of cortical activation. These results were validated for different oxygen saturations, wavelength combinations and scattering coefficients. For the analysis of changes in oxygenated and deoxygenated hemoglobin only, low cross talk was also found when the activated volume was assumed to be a 4-mm-diam sphere. © *2002 Society of Photo-Optical Instrumentation Engineers.* [DOI: 10.1117/1.1427048]

Keywords: near-infrared spectroscopy; Monte-Carlo simulation; functional activity of the brain; cross talk; cytochrome-c-oxidase.

1 Introduction

Changes in the optical properties of biological tissues can be determined with near-infrared spectroscopy (NIRS) operating in the wavelength range from 650 to 950 nm. NIR light can penetrate the adult skull and thus can be used to noninvasively examine functional activity of the brain.[1] Since it is currently impossible to compare concentration changes determined noninvasively with real changes occurring during functional activation of the brain, theoretical models have to be used to estimate possible errors in the determination of chromophore changes.

For a given spatial inhomogeneous absorption change, the magnitude of the concentration changes using the modified Lambert-Beer law (MLBL) is underestimated, because the activated volume is smaller than the sampling volume.[2] This is generally referred to as partial volume effect. Matters are further complicated by the wavelength dependence of the optical tissue properties resulting in a wavelength dependence of this partial volume effect, which leads to a cross talk between the chromophores.

If multiple chromophores are to be determined, a change in one of the chromophores may mimic a change in another chromophore. This issue is of supreme importance when including chromophores with greatly different concentration changes in the sampled tissue, as in the case of cytochrome-c-oxidase, whose concentration changes is at least an order of magnitude smaller than that of the hemoglobins. To address the above issues, the present paper proceeds from a

1. Monte Carlo (MC) simulation on a layered structure to calculate the photon pathlength in each layer. Special considerations were made to mimic the optical properties of the adult human head.

2. We next introduced inhomogeneous chromophore concentration changes leading to a change in attenuation. From this attenuation change we determined concentration changes with MLBL, thus allowing to compare them with the introduced concentration changes.

3. The resulting cross talk for changes in oxygenated hemoglobin, deoxygenated hemoglobin and the redox state of cytochrome-c-oxidase was tested for different assumed tissue properties, wavelength combinations and location of the induced chromophore changes. To investigate the different sensitivity of intensity and mean time of flight measurements, we also determined concentration changes using changes in mean time of flight instead of attenuation.

4. While most of the results are discussed for homogeneous tissue models with chromophore changes restricted to a single layer, an inhomogeneous-layered head model[2] and focal changes were explored as well.

Address all correspondence to Kamil Uludag. Tel: 49-30-450-560075; Fax: 49-30-450-560952; E-mail: kamil.uludag@charite.de

The issue of erroneous chromophore calculations has been addressed before by Matcher et al.[3] who focused on homogeneous absorption changes throughout the tissue and optimization of algorithm by choice of wavelengths and (total) mean photon pathlength. Similarly, this topic is covered by Mayhew et al.[4] and Kohl et al.[5] for reflected light of the open cortex in the visible wavelength range. The recent paper by Boas et al.[6] indicates the importance of the relative position of the focal activation with respect to source and detector.

2 Theory

Light attenuation A is defined as:

$$A = -\ln(I/I_0). \tag{1}$$

Here I_0 is the incident intensity (proportional to the number of injected photons per unit time), and I the measured intensity (proportional to the number of detected photons per unit time).

For a turbid medium and light in the near-infrared wavelength range it has been proposed[7] that a small homogeneous change in the absorption coefficient $\Delta\mu_a [\mathrm{mm}^{-1}]$ leads to a change in the attenuation

$$\Delta A(\lambda) = L(\lambda) \cdot \Delta\mu_a(\lambda). \tag{2}$$

Here L is the effective pathlength of the photons at wavelength λ. Due to multiple light scattering L is larger than the source-detector distance r. $\Delta\mu_a$ is related to a concentration change $\Delta c [\mu M]$ of chromophores by

$$\Delta\mu_a(\lambda) = \ln(10) \cdot \sum_i \epsilon_i(\lambda) \cdot \Delta c_i. \tag{3}$$

The term ϵ is the decadic extinction coefficient $[OD\ \mu M^{-1}\ mm^{-1}]$ and i labels the different chromophores. Equations (2) and (3) are the basis of a spectroscopic analysis of hemoglobin and cytochrome-c-oxidase changes from multi-wavelengths attenuation data.

Similar to the above analysis for attenuation data, changes in mean time of flight of the photons $\langle t \rangle$ can be exploited to calculated chromophore concentration changes in homogeneous media for small absorption changes

$$\Delta\langle t\rangle(\lambda) = \Delta\mu_a(\lambda) \cdot [\langle t\rangle^2(\lambda) - \langle t^2\rangle(\lambda)] \cdot \nu_n. \tag{4}$$

The term ν_n is the velocity of light in tissue. The factor $(\langle t\rangle^2 - \langle t^2\rangle) \cdot \nu_n$ is the specialization of the mean time sensitivity factor (MTSF)[8] for homogeneous changes in μ_a. MTSF is equivalent to the differential mean time factor calculated by Firbank, Okada, and Delpy[9] with finite element methods for an adult human head.

Equations (2) and (4) are valid for homogeneous changes only. In case of an inhomogeneous change in μ_a, an equation similar to Eq. (2) [or Eq. (4)] can be applied. It has been shown by Hiraoka et al.[10] that the total attenuation change is the sum of the attenuation changes induced by absorption changes in all partial volumes $\Delta\mu_{a,j}$

$$\Delta A(\lambda) = \sum_j l_j(\lambda) \cdot \Delta\mu_{a,j}(\lambda). \tag{5}$$

The effective partial pathlength l_j in the partial volume labeled with j replaces the effective total pathlength L [see Eq. (2)]. An analogous equation can be formulated for changes in mean time of flight in partial volumes.[8]

The assumption of a homogeneous change is often made because the partial pathlengths can only be estimated, while the total pathlength can be measured with frequency-domain or time-resolved instruments.[11–13] The question is: how accurate is an analysis based on Eq. (2) [or Eq. (4)] if the change in the absorption coefficient of the tissue is inhomogeneous.

Absorption changes induced in partial volumes affect the calculated absorption changes in two ways: First, the magnitude of absorption changes (i.e., chromophore changes) is underestimated.[2] Second, cross talk between the chromophores results in a false calculation of chromophore changes.

The reason for the cross talk is that the penetration depth and therefore the partial pathlength l_j depends on absorption and scattering properties of the tissue. Inhomogeneous μ_a changes modify the measured quantities (ΔA or $\Delta\langle t\rangle$) due to the wavelength dependence of the partial pathlengths. Consequently, the determined changes in the chromophores using Eq. (2) [or Eq. (4)] with measured or assumed $L(\lambda)$ [or MTSF(λ)] can differ from the induced changes.

To illustrate this issue, a medium is considered in which a concentration change is induced in only one chromophore ($\Delta c_{a,\mathrm{ind}}$) in a single partial volume. Using $l_j^* = l_j/L$ as the relative partial pathlength and two wavelengths (λ_1, λ_2) only, using Matrix inversion the calculated concentration changes in chromophores a and b ($\Delta c_a, \Delta c_b$) can be derived as

$$\frac{\Delta c_a}{\Delta c_{a,\mathrm{ind}}}$$

$$= \frac{\epsilon_a(\lambda_1) \cdot \epsilon_b(\lambda_2) \cdot l_j(\lambda_1)^* - \epsilon_a(\lambda_2) \cdot \epsilon_b(\lambda_1) \cdot l_j(\lambda_2)^*}{\epsilon_a(\lambda_1) \cdot \epsilon_b(\lambda_2) - \epsilon_a(\lambda_2) \cdot \epsilon_b(\lambda_1)}, \tag{6}$$

$$\frac{\Delta c_b}{\Delta c_{a,\mathrm{ind}}} = \frac{\epsilon_a(\lambda_1) \cdot \epsilon_a(\lambda_2) \cdot (l_j(\lambda_2)^* - l_j(\lambda_1)^*)}{\epsilon_a(\lambda_1) \cdot \epsilon_b(\lambda_2) - \epsilon_a(\lambda_2) \cdot \epsilon_b(\lambda_1)}. \tag{7}$$

Δc_b is proportional to the difference of the relative partial pathlengths $(l_j(\lambda_2)^* - l_j(\lambda_1)^*)$. For small differences in $l_j(\lambda)^*$ the calculated Δc_a is $l_j(\lambda)^* \cdot \Delta c_{a,\mathrm{ind}}$.

We define the cross talk $C_{a\to b}$ from chromophore a to chromophore b as the ratio of the determined concentration change of the chromophore b, for which no change was induced, and the determined concentration change of the chromophore a, for which the change was induced. Using two wavelengths and the same assumptions as above leads to

$$C_{a\to b}$$

$$= \frac{\epsilon_a(\lambda_1) \cdot \epsilon_a(\lambda_2) \cdot (l_j(\lambda_2)^* - l_j(\lambda_1)^*)}{\epsilon_a(\lambda_1) \cdot \epsilon_b(\lambda_2) \cdot l_j(\lambda_1)^* - \epsilon_a(\lambda_2) \cdot \epsilon_b(\lambda_1) \cdot l_j(\lambda_2)^*}. \tag{8}$$

Because only small changes are assumed, the cross talk is independent of the magnitude of the induced change $\Delta c_{a,\text{ind}}$ that acts as a scaling factor. Note that the cross talk $C_{a \to b}$ is different from $C_{b \to a}$ in magnitude and sign.

3 Methods

3.1 Monte Carlo Simulation

To determine the cross talk using absorption changes in a layered model of the adult human head, MC simulations were performed.

The simulations were calculated using a model with homogeneous layers labeled by j. The medium was composed of ten layers with the upper nine layers having a thickness of 2 mm and the deepest layer being semi-infinite. Either all layers had the same reduced scattering coefficient $\mu'_{s,j}$ (1 or 2 mm^{-1}) or they had a wavelength dependent $\mu'_{s,j}$ as calculated for the adult head by Matcher, Cope, and Delpy[14] with values given by $\mu'_s(\lambda) = a \cdot \lambda + b$ ($a = -6.5 \times 10^{-4}$ mm^{-1} nm^{-1}, $b = 1.45$ mm^{-1}). In the homogeneous head model all layers had the same (wavelength dependent) absorption coefficient $\mu_{a,j}$. For $\mu_{a,j}$ 19 different values from 0.010–0.070 mm^{-1} were used to cover the range expected over the NIR spectral band used in tissues.

To investigate focal changes we used the homogeneous head model and introduced absorption changes in spheres of radius 2 mm (sphere model), which were positioned at various depth and distances with respect to source and detector. In addition to the homogeneous head model, the more complex head model of Okada et al.[2] was investigated.

Scattering anisotropies were disregarded. We assumed the same refractive index $n = 1.4$ for all layers. Fresnel reflection at the tissue–air boundary was disregarded, i.e., the boundary was totally absorbing.

The MC simulation based on the variance reduction technique is described elsewhere in detail.[8,10] In brief, the pathlength in each layer and the survival weight were calculated for each photon. The photons were detected in concentric rings differing by 3 mm in diameter. The middle radius r of these rings was varied from 6 to 60 mm. For focal changes photons were detected in a ring segment with a fractional outer circumference of 2 mm length. The time-independent partial pathlength l_j for every layer was obtained by integrating the product of the time-dependent photon pathlengths and the normalized distribution of time of flight (for the details of the averaging method see Ref. 8).

For all layers the standard deviation of l_j was determined for different μ_a values by performing 30 runs of the MC simulation and was found to be smaller than 1.5% for a source-detector distance of 30 mm. The standard deviation of MTSF$_j$ was determined to be smaller than 7% for the layers in the depth from 4 to ∞ mm.

For the homogeneous head model 4.2×10^7 photons were injected. For the more complex head model based on Okada et al.,[2] 2×10^8 and for the sphere model 2.5×10^9 photons were used.

3.2 μ_a–λ relationship

The composition of the model tissue has to be assumed because for a spectroscopic analysis $l_j(\lambda)$ rather than $l_j(\mu_a)$ is needed.
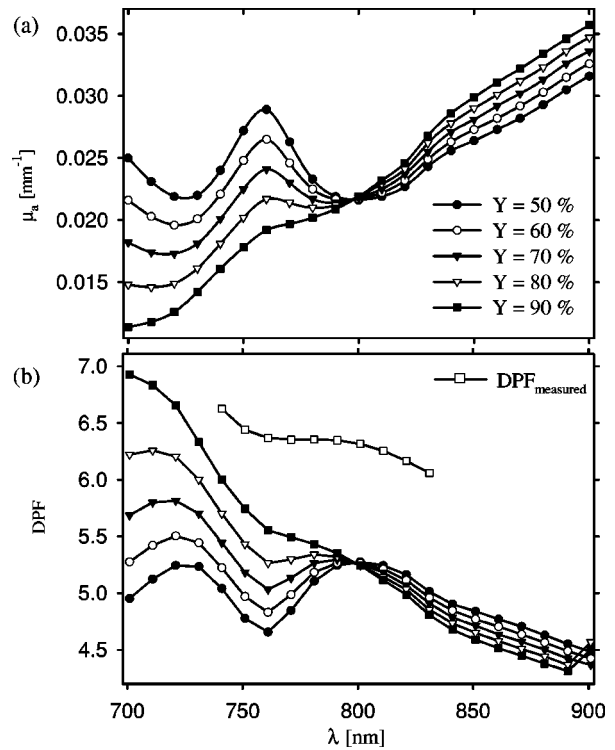

Fig. 1 (a) Absorption coefficient μ_a and (b) calculated DPF for different oxygen saturations Y as a function of wavelength λ. For the tissue model a total hemoglobin concentration of 100 μM and $\mu'_s = 1$ mm^{-1} was assumed. To allow a comparison of the DPF $= L/r$ with experimental values taken from Essenpreis et al.[12] (open squares) a source-detector distance of $r = 40$ mm was used.

A water fraction of 90% (vol.) was assumed, which is the average water concentration in the neonatal brain.[7] Because of the small μ_a of water in the so-called "optical window" (700–900 nm) a variation of the water concentration has little effect on the resulting μ_a of the tissue. For simplicity other chromophores than hemoglobin like fat and lipids were neglected.[7]

The total hemoglobin concentration of the brain is approximately 100 μM.[7,14] This value was adopted in the model. For the oxygen saturation $Y = \text{Oxy-Hb}/(\text{Oxy-Hb} + \text{Deoxy-Hb})$ values between $Y = 50\%$ and 90% were regarded. Here Oxy-Hb and Deoxy-Hb symbolize the concentration of the oxygenated and deoxygenated hemoglobin. The resulting absorption coefficient μ_a is consequently

$$\mu_a = 0.9 \cdot \mu_{a,\text{water}} + 100 \mu\text{M} \cdot \ln(10) \cdot (Y \cdot \epsilon_{\text{Oxy-Hb}} + (1 - Y)$$
$$\cdot \epsilon_{\text{Deoxy-Hb}}). \tag{9}$$

The $\mu_{a,\text{water}}$ was calculated from water extinction coefficients given by Ref. 15. The $\epsilon_{\text{Oxy-Hb}}$ and $\epsilon_{\text{Deoxy-Hb}}$ were taken from Ref. 16. In Figure 1(a) the resulting wavelength dependent absorption coefficients are shown for the different saturation values.

The relative maximum of the extinction of deoxygenated hemoglobin around 760 nm can be seen in the resulting μ_a spectra. The values of μ_a at 800 nm ($\mu_a \sim 0.021$ mm^{-1}) are in agreement with the literature, where values ranging from 0.016 to 0.021 mm^{-1} are reported for the adult head.[9,14] Bev-
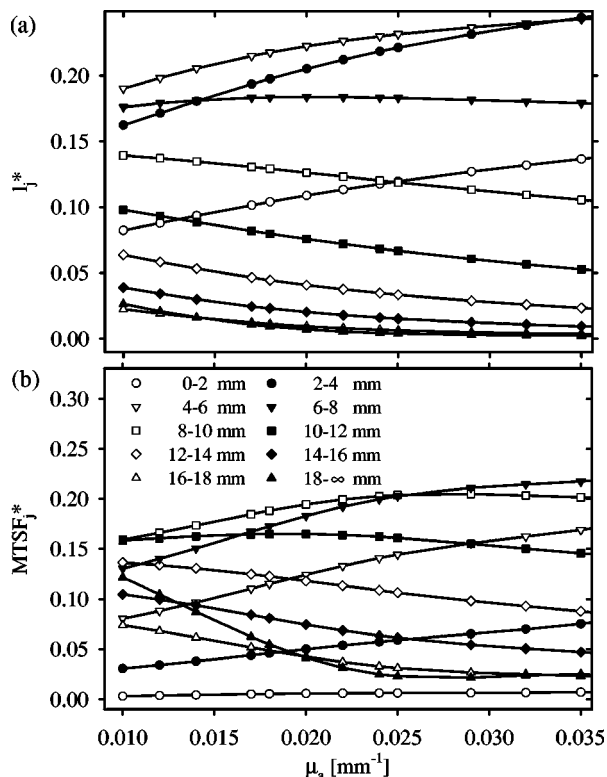
Fig. 2 (a) Relative partial pathlength l_j^* and (b) relative partial mean time sensitivity factor $MTSF_j^*$ as a function of absorption coefficient μ_a for different layers of 2 mm thickness. For the calculations $\mu_s' = 1$ mm^{-1} and $r = 30$ mm are assumed.

Fig. 3 Determined ΔOxy-Hb and ΔDeoxy-Hb from changes in attenuation ΔA and mean time-of-flight $\Delta\langle t\rangle$ for induced (a) ΔOxy-Hb $= 1$ μM and (b) ΔDeoxy-Hb $= 1$ μM. The entire wavelength range from 700 to 900 nm (multi λ) or only two wavelengths at 760 and 830 nm (2 λ) are used. The assumed saturation is $Y = 70\%$. Note that in (a) ΔDeoxy-Hb and in (b) ΔOxy-Hb are scaled by a factor of 5. The gray box indicates the most likely depth for cortical activity.

ilacqua et al.[17] measured absorption coefficients of various cortical tissues including skull and found μ_a values in the range 0.018–0.022 mm^{-1}.

A direct way to check the assumed tissue parameters is the comparison of experimental time-of-flight measurements with total pathlengths calculated from the model. The pathlength divided by the source-detector distance (called differential pathlength factor DPF$= L/r$) is frequently used in the literature.

Experimental DPF values taken from Ref. 12 for $r = 40$ mm and the calculated DPF from the model tissue using the same r and $\mu_s' = 1$ mm^{-1} are shown in Figure 1(b). The measured and the calculated wavelength dependence of the DPF are similar, especially for saturation values under physiological conditions ($Y = 70\% - 90\%$). The magnitude of the measured DPF is about 20% greater than the calculated one, however, this deviation is smaller than the intraindividual variations.[12]

4 Results

4.1 Relative Partial Pathlength (l_j^*) and Relative Partial Mean Time Sensitivity Factor ($MTSF_j^*$)

Figure 2 shows the relative partial pathlength l_j^* and the relative partial mean time sensitivity factor $MTSF_j^*$ as a function of the absorption coefficient μ_a. The quantity $MTSF_j^*$ is the ratio of the partial to total mean time sensitivity factor. Here a commonly used source detector distance of $r = 30$ mm was
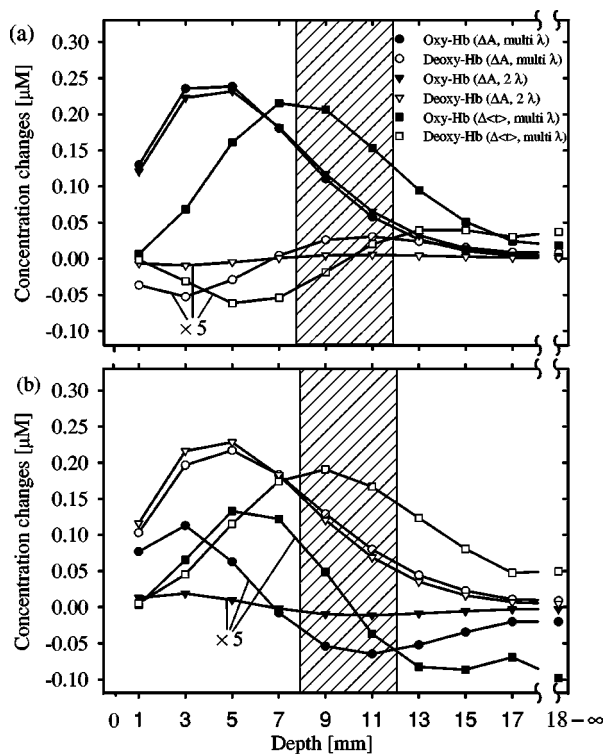
chosen; $\mu_s' = 1$ mm^{-1} was used. The different layers are indicated by different symbols. The absorption coefficient was varied between $\mu_a = 0.010$ and 0.0360 mm^{-1} which is approximately the range given in Figure 1(a). Based on these values and a fifth order polynomial, l_j^* and $MTSF_j^*$ were approximated as a function of μ_a.

The objective of this publication is focused on cortical absorption changes in the adult head, thus l_j^* and $MTSF_j^*$ in the layers at depths of 8–12 mm are of special relevance. In this region of interest l_j^* varies up to a factor of 2 and $MTSF_j^*$ by less than 25% within the range of regarded μ_a. $MTSF_j^*$ is very small for the layer from 0 to 2 mm and the noise level is consequently high. Therefore no concentration changes of the chromophores are determined from $\Delta\langle t\rangle$ for this layer.

4.2 Homogeneous Layered Model

Figure 3 shows the determined concentration changes for induced changes of 1 μM in Oxy-Hb [Figure 3(a)] and Deoxy-Hb [Figure 3(b)]. The corresponding cross talk is plotted in Figures 4 and 5. To compare the depth sensitivity of intensity and mean time spectroscopy, chromophore changes were derived from both ΔA and $\Delta\langle t\rangle$. The induced changes were restricted to single layers, which are indicated by their corresponding mean depth. Based on the standard deviation of l_j (or $MTSF_j$) an uncertainty in the calculated concentration changes smaller than 3% (or 14%) is estimated.
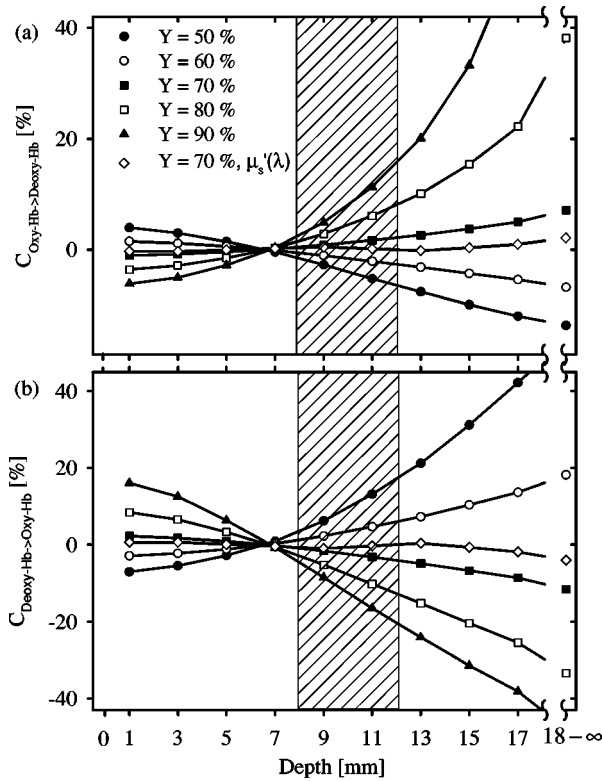
Fig. 4 Cross talk determined from changes in attenuation ΔA in % as a function of depth of the activated layer with induced (a) ΔOxy-Hb or (b) ΔDeoxy-Hb$=1$ μM for different oxygen saturations Y using wavelengths at 760 and 830 nm; $\mu_s'=1$ mm^{-1} was assumed. For the case $Y=70\%$ additionally a wavelength dependent $\mu_s'(\lambda)$ was chosen. The gray box indicates the most likely depth for cortical activity.
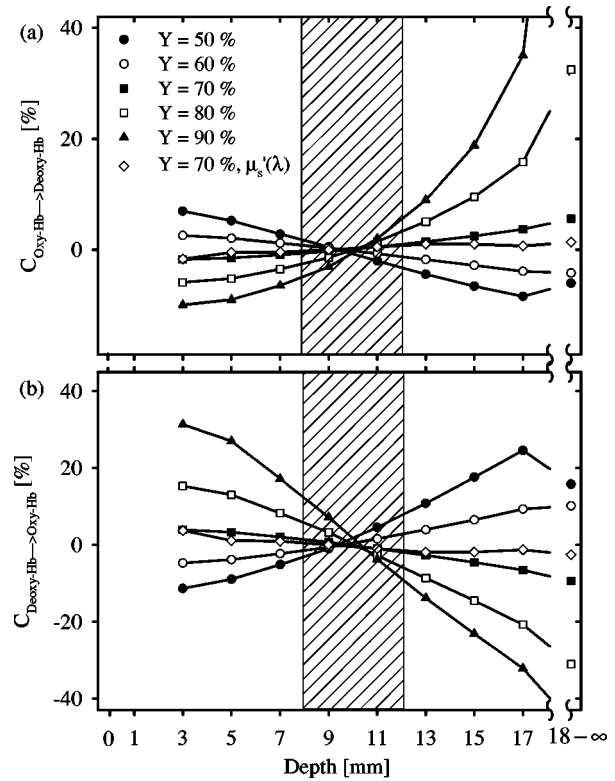
Fig. 5 Cross talk determined from changes in mean time-of-flight $\Delta\langle t\rangle$ in % as a function of depth of the activated layer with induced (a) ΔOxy-Hb or (b) ΔDeoxy-Hb$=1$ μM for different oxygen saturations Y using wavelengths at 760 and 830 nm; $\mu_s'=1$ mm^{-1} was assumed. For the case $Y=70\%$ additionally a wavelength dependent $\mu_s'(\lambda)$ was chosen. The gray box indicates the most likely depth for cortical activity.

For the analysis we used either the entire wavelength range (700–900 nm) or two wavelengths commonly used for hemoglobin spectroscopy (760 and 830 nm). While in the latter case Eqs. (6) and (8) give an analytical solution, for the multiwavelengths case a least squares fitting routine was employed to calculate concentration changes from spectra of $\Delta A(\lambda)$ or $\Delta\langle t\rangle(\lambda)$. The scattering coefficient was set to $\mu_s'=1$ mm^{-1} and a saturation of $Y=70\%$ was assumed.

For the case of the entire wavelength range, induced changes in the region of interest (8–12 mm) in Oxy-Hb of 1 μM [Figure 3(a)] leads to determined ΔDeoxy-Hb up to ~0.006 μM and to determined ΔOxy-Hb up to ~0.12 μM. The cross talk for these layers is below $\sim11\%$. Using only the two mentioned wavelengths for the analysis, this cross talk is about 2%. For induced changes in Deoxy-Hb of 1 μM and focusing on the same layers (8–12 mm), using the entire wavelength range the magnitude of the cross talk is below $\sim17\%$. Again, based on the two wavelength analysis, the magnitude of the cross talk ($\sim3\%$) is much smaller.

When determined from $\Delta\langle t\rangle$ rather than ΔA, the maximum of ΔOxy-Hb as well as the minimum of the magnitude of the cross talk are in deeper layers. In the layers from 2 to 8 mm the magnitude of the cross talk calculated with $\Delta\langle t\rangle$ is bigger than calculated with ΔA, for deeper layers it is smaller (see Figures 4 and 5).

Using ΔA, the cross talk determined for two wavelengths 760 and 830 for induced changes in Oxy-Hb [Figure 4(a)] and

Deoxy-Hb [Figure 4(b)] are different in magnitude and sign. For 70% saturation the cross talk is almost zero for all layers because the difference in the absorption coefficient is small [compare with Figure 1(a)]. For saturations of 80% and 90% the cross talk is significant in deep layers for an induced change in Oxy-Hb [Figure 4(a)]. Given a change in Deoxy-Hb, the cross talk is high for saturation values of 50%, 80% and 90% [Figure 4(b)]. At a depth of approximately 7 mm, the cross talk is close to zero almost independent of the saturation value.

The cross talk determined with $\Delta\langle t\rangle$ based on 760 and 830 nm is shown in Figure 5 for induced changes in Oxy-Hb and Deoxy-Hb. For each saturation value the magnitude of the cross talk in the region of interest (8–12 mm) is smaller than determined with ΔA. As the cross talk depends on the differences in absorption coefficient [Figure 1(a)], partial pathlength and partial mean time sensitivity factor (Figure 2), the cross talk is crucially dependent on the wavelength combination and the saturation value.

When including a reduced scattering coefficient $\mu_s'(\lambda)$ which linearly decreases with wavelength (see Method section) and assuming a saturation of $Y=70\%$, for induced Oxy-Hb [Figures 4(a) and 5(a)] and Deoxy-Hb changes [Figures 4(b) and 5(b)] the magnitude of the cross talk for all layers is smaller than 4%. For the region of interest (8–12 mm) the magnitude of the cross talk determined from ΔA (or
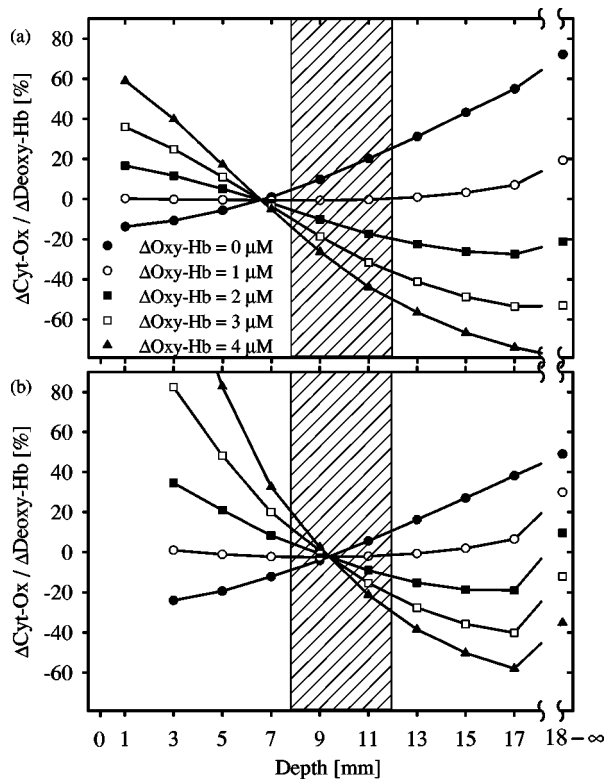
Fig. 6 Ratio of determined Δ Cyt-Ox to ΔDeoxy-Hb from changes in (a) attenuation ΔA and (b) mean time-of-flight $\Delta\langle t\rangle$ as a function of depth of the activated layer for different values of induced ΔOxy-Hb and a fixed ΔDeoxy-Hb of -1 μM. $Y=70\%$, $\mu_s'=1$ mm^{-1} and a source-detector distance of $r=30$ mm is assumed. A wavelength range 700–900 nm is considered. The gray box indicates the most likely depth for cortical activity.

$\Delta\langle t\rangle$) with wavelength dependent μ_s' is smaller than determined with a constant μ_s'.

Changing the magnitude of the scattering coefficient from $\mu_s'=1-2$ mm^{-1} has only an insignificant effect on the cross talk (data not shown). For a greater source-detector separation r, the sensitivity of attenuation and mean time-of-flight measurements is in deeper layers. However, the magnitude of the cross talk remains in the same order (data not shown).

So far, only changes in Oxy-Hb and Deoxy-Hb were considered. The question arises if determined concentration changes in cytochrome-c-oxidase (ΔCyt-Ox) can be due to the cross talk artifact. During visual stimulation experiments using an analysis based on MLBL, an increase in Oxy-Hb, decrease in Deoxy-Hb and a simultaneous increase in Cyt-Ox was obtained.[18,19] To cover the observed concentration changes in our model, we induced different values of ΔOxy-Hb (0–4 μM) while the decrease in ΔDeoxy-Hb was fixed at -1 μM. Again, the assumed saturation is 70% and $\mu_s'=1$ mm^{-1}. From the attenuation changes (700–900 nm) induced by the hemoglobin changes, ΔOxy-Hb, ΔDeoxy-Hb as well as ΔCyt-Ox were calculated with Eqs. (2) and (3). In Figure 6 the determined ratio of ΔCyt-Ox/ΔDeoxy-Hb from changes in (a) attenuation ΔA and (b) mean time of flight $\Delta\langle t\rangle$ is shown as a function of the depth of the activated layer.

For induced ΔOxy-Hb$=1$ μM the determined ΔCyt-Ox/ΔDeoxy-Hb is small for all layers—except for the semi-
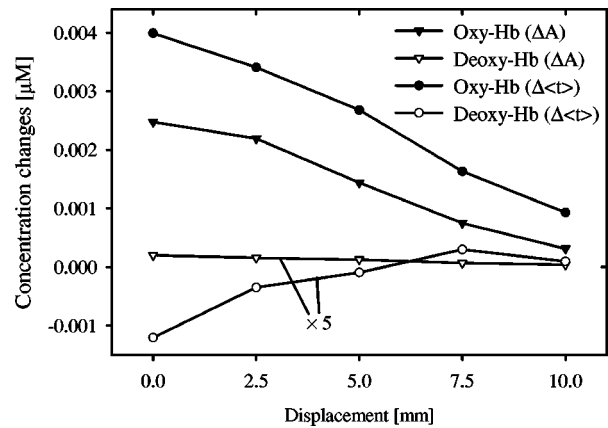

Fig. 7 Determined changes of Oxy-Hb and Deoxy-Hb from changes in attenuation ΔA and mean time-of-flight $\Delta\langle t\rangle$ induced by ΔOxy-Hb$=1$ μM in a sphere as a function of the displacement perpendicular from the line between source and detector. The center of the sphere of radius 2 mm is located at a depth of 10 mm. For zero displacement the sphere is positioned under the midpoint of the line connecting source and detector (distance 27 mm). $Y=70\%$, $\mu_s'=1$ mm^{-1} is assumed. The wavelengths used are 760 and 830 nm. Note that ΔDeoxy-Hb is scaled by a factor of 5.

infinite layer determined from $\Delta\langle t\rangle$. At the depth of $\sim$6 mm ($\sim$9 mm) ΔCyt-Ox/ΔDeoxy-Hb determined from ΔA ($\Delta\langle t\rangle$) is zero for all values of induced ΔOxy-Hb. For a pure Deoxy-Hb change in the tissue (ΔOxy-Hb$=0$ μM), a spurious Cyt-Ox change determined from ΔA as well as from $\Delta\langle t\rangle$ up to 20% of the Deoxy-Hb change is estimated for cortical layers (8–12 mm). For larger ΔOxy-Hb, the derived magnitude of the ratio ΔCyt-Ox/ΔDeoxy-Hb is even bigger.

Using the same model and an analysis with different combinations of three or four wavelengths, the magnitude of the determined ratio ΔCyt-Ox/ΔDeoxy-Hb is bigger than 30% for at least one of the induced Oxy-Hb values (data not shown).

4.3 Focal Changes

In the models considered so far, the hemoglobin changes are restricted to whole layers of the head. This is certainly a coarse assumption for functional activations for which focal changes are more realistic. For this reason we also investigated induced changes in spheres. For the data of Figure 7 the center of the spheres of 2 mm radius are located at a depth of 10 mm. The different spheres are displaced 0–10 mm perpendicular to the source-detector connection line. For zero displacement the sphere is positioned under the midpoint of this connection line (source detector distance 27 mm). The same wavelengths as above (760 and 830 nm) and a saturation value of $Y=70\%$ are used. In Figure 7 ΔOxy-Hb and ΔDeoxy-Hb determined from changes in attenuation ΔA and mean time-of-flight $\Delta\langle t\rangle$ are presented induced by ΔOxy-Hb$=1$ μM in the spheres. The results for induced changes in Deoxy-Hb are qualitatively similar and therefore not shown. With increased displacement the observed concentration change gets smaller. ΔOxy-Hb determined from $\Delta\langle t\rangle$ is $\sim$1.5 times greater than determined from ΔA for zero displacement and $\sim$3 times greater for 10 mm displacement. The corresponding cross talk determined from ΔA ($\Delta\langle t\rangle$) is smaller than 2.5% (6%) for all displacements chosen.

Table 1 Thickness, absorption coefficient μ_a and scattering coefficient μ_s' taken from Ref. 2 for different parts of a layered head model (for CSF μ_a of water is used).

	Thickness (mm)	μ_a (mm^{-1})	μ_s' (mm^{-1})
Skin/skull	10	0.04	2.0
CSF	2	0.0034	0.01
Gray matter	4	0.025	2.5
White matter	Semi-infinite	0.005	6.0

4.4 Layered Brain Model

Above, the brain is modeled in a crude fashion using the same optical properties in all layers. Okada et al.[2] have developed a more realistic model including different absorption and scattering properties for the different tissues of the head. We adopted this model with the optical properties given in Table 1. For μ_a of the cerebrospinal fluid (CSF) we used the absorption coefficient of water at 830 nm instead of 0.001 mm^{-1}.[2]

For this head model, the cross talk was calculated at two wavelengths (760 and 830 nm). The wavelength dependence of μ_a was included by assuming that the absorption coefficients of Table 1 are valid at $\lambda = 830$ nm and due to water and the two hemoglobin fractions. Based on the same water content (90%) and the same saturation $Y = 70\%$, absolute hemoglobin concentrations were derived for each layer and subsequently absorption coefficients at 760 nm: $\mu_a = 0.0381$ mm^{-1} for skin/skull, 0.0236 mm^{-1} for gray matter and 0.0046 mm^{-1} for white matter. Again for CSF the absorption coefficient of water (0.0029 mm^{-1}) was used. A wavelength independent μ_s' was assumed.

In Figure 8 determined ΔOxy-Hb and ΔDeoxy-Hb values from ΔA and $\Delta\langle t\rangle$ are shown for induced changes ΔOxy-Hb $= 1$ μM. (For induced ΔDeoxy-Hb $= 1$ μM similar
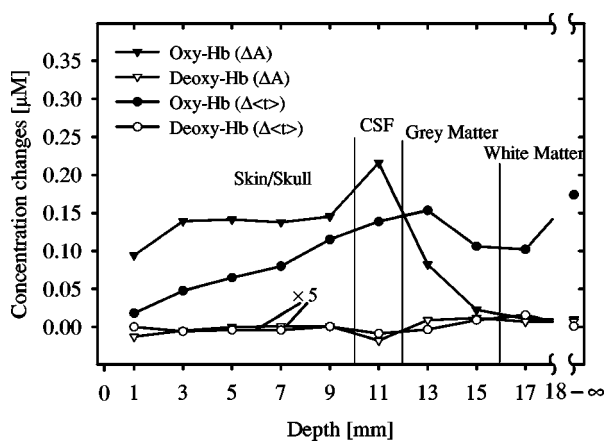

Fig. 8 Determined changes in Oxy-Hb and Deoxy-Hb from changes in attenuation ΔA and mean time-of-flight $\Delta\langle t\rangle$ in an inhomogeneous layered brain model and induced ΔOxy-Hb $= 1$ μM. Wavelengths at 760 and 830 nm and for source-detector distance $r = 27$ mm were used. The optical properties of the layers are given in Table 1 for 830 nm. Note that ΔDeoxy-Hb is scaled by a factor of 5.

results were obtained.) Although a change of 1 μM in the CSF layer is not a physiological plausible value, here it was chosen for consistency. As before for the layered homogeneous model, the magnitude of the calculated changes reflects the pathlength contribution of the different layers. The Oxy-Hb signal determined from ΔA peaks for the CSF. This is explained by the ''light pipe'' properties of the CSF.[2] For the skin/skull and CSF layers the determined ΔOxy-Hb from ΔA is greater than determined from $\Delta\langle t\rangle$, for the other layers it is smaller.

The magnitude of the cross talk determined from ΔA is smaller than 3% for skin and skull and the upper part of the gray matter (depth 12–14 mm). For deeper layers it goes up to 14%. However, as the magnitude of the determined chromophore changes is very small for these layers, this cross talk is probably of no significance in real measurement conditions. The magnitude of the cross talk determined from $\Delta\langle t\rangle$ is smaller than 4% for all layers.

To test for possible Cyt-Ox artifacts, four wavelengths (750, 830, 850 and 925 nm) were included in the analysis. These are the same used by Heekeren et al.[18] and close to those of a commercial NIRS monitor (NIRO-500, Hamamatsu Photonics K.K., Japan). For 750, 850, and 925 nm the absorption coefficient was derived from Table 1 in the same fashion as for 760 nm. Inducing different ratios of ΔOxy-Hb and ΔDeoxy-Hb (as in Figure 6) in the upper gray matter layer returns a ratio ΔCyt-Ox/ΔDeoxy-Hb determined from ΔA ($\Delta\langle t\rangle$) which is smaller by a factor of 2 (4) compared to using the homogeneous layered model same depth 12–14 mm and same wavelengths (data not shown).

5 Discussion

The cross talk in the calculation of chromophores depends on the tissue's optical properties and their wavelength dependence. We therefore tried to adapt the model properties (μ_a, μ_s') to mimic experimentally accessible data. Saturation values between 50% and 90% were assumed [see Figure 1(a)]. For different saturation values, the mean optical pathlength of our model tissue is in overall agreement with experimental measurements in volunteers [see Figure 1(b)]. In addition, the wavelength dependence of the attenuation spectrum roughly matches that measured in volunteers (data not shown).[3]

Here we focus on standard measurement configurations with a single light source and a single detector. In the simplest case two common wavelengths (i.e., 760 and 830 nm) for hemoglobin spectroscopy were considered. Besides that, different spectral ranges between 700 and 900 nm were taken into account allowing Cyt-Ox changes to be included.

The model for the cross talk estimation proposed here is straightforward. First, changes in attenuation or mean time of flight were calculated for chromophore changes restricted to a partial volume of the model tissue. For that, the partial pathlength (l_j) and the partial mean time sensitivity factor (MTSF$_j$) were derived from MC simulations for layered models (see Figure 2) and for a sphere in a semi-infinite medium. The concept of relative partial pathlengths (l_j^*) proposed here directly corresponds to the approximation terms given in Ref. 6. Second, the chromophore changes were recalculated with the modified Lambert-Beer law based on

knowledge of the experimentally accessible data (total pathlength). As a consequence, erroneous calculations of chromophore concentration changes appear due to a partial volume effect and its wavelength dependence.

Bearing in mind the assumptions of the model, there are conclusions to be drawn for NIRS spectroscopy of tissue. First of all, it needs to be stressed that for global changes as encountered, e.g., in muscle studies or in physiological challenges[20,21] like hypoxia or hypercapnia the cross talk is small. This can be seen in Figures 3 and 8 by adding the concentration changes of the upper layers up to the estimated depth.

The main points of interest here are functional activation studies in adults where the chromophore changes are mostly restricted to the gray matter, i.e., the likely depth is around 10 mm. This value varies for volunteers and site, with, e.g., a thicker skull over the visual cortex compared with the motor cortex. In Figures 3–6 this depth (8–12 mm) is indicated. In the model proposed by Okada et al.[2] and adapted here (Figure 8), the gray matter is somewhat deeper.

For this depth the cross talk between the hemoglobin components is estimated to be a few percent only up to 10% depending on the assumptions made (Figures 3–5). It is demonstrated that the relative higher depth sensitivity of mean time-of-flight data results in lower cross talk for these tissue layers.

The model predicts that changes in deep cortical areas might have cross talk unacceptably high for functional studies. For example, for a depth of 17 mm and saturation values of 80%, the cross talk is >20% (Figure 4). However, the partial pathlength is very small [<3% for the layer of 16–18 mm, see Figure 2(a)] and therefore the absolute magnitude of the concentration change is most likely to be insignificant in real measurement conditions (Figure 3). That is, the high cross talk might have hardly any significance in practical terms for quantification of hemoglobin.

To allow a better comparison with Boas et al.,[6] who recently pointed out the shortcomings of the modified Lambert-Beer law, we extended our model from activated layers to activated spheres of radius 2 mm at a depth of 10 mm (Figure 7). For induced focal changes in hemoglobin at different locations with respect to source and detector, the cross talk is only a few percent.

In summary, when only oxygenated and deoxygenated hemoglobin are regarded, the estimated cross talk is small for the relevant cases. However, this result has to be experimentally validated for different measurement conditions.

Recently we presented the analysis of visual stimulation experiments in adults claiming a transient increase in the redox state of cytochrome-c-oxidase concurrent with the hemoglobin response.[18] Being aware that the separation of the hemoglobin and the redox state of cytochrome-c-oxidase signals might be a problem, we ensured the stability of the signals when applying various wavelength ranges from established four wavelengths to continuous spectra.[4] The estimations presented here question these findings: when assuming changes in oxygenated hemoglobin and deoxygenated hemoglobin commonly detected in activation studies, the magnitude of the erroneously determined changes in the redox state of cytochrome-c-oxidase (Figure 6) might be in the order of those detected experimentally.[18]

Experimental solutions to avoid or minimize cross talk are not apparent. As mentioned by Boas et al.,[6] imaging with a multisource-multidetector device might reduce some of the problem, however, this has not been proven experimentally. Inclusion of time-of-flight information might additionally vindicate concentrations calculated by attenuation data, as both parameters probe different depths with lowest cross talk (Figures 3–8).

References

1. A. Villringer and B. Chance, "Non-invasive optical spectroscopy and imaging of human brain function," *Trends Neurosci.* **20**, 435–442 (1997).
2. E. Okada, M. Firbank, M. Schweiger, S. R. Arridge, M. Cope, and D. T. Delpy, "Theoretical and experimental investigation of near infrared light propagation in a model of the adult head," *Appl. Opt.* **36**, 21–31 (1997).
3. S. J. Matcher, C. E. Elwell, C. E. Cooper, M. Cope, and D. T. Delpy, "Performance comparison of several published tissue near-infrared spectroscopy algorithms," *Anal. Biochem.* **227**, 54–68 (1995).
4. J. Mayhew, Y. Zheng, Y. Hou, B. Vuksanovic, J. Berwick, S. Askew, and P. Coffey, "Spectroscopic analysis of changes in remitted illumination: the response of increased of neural activity in brain," *Neuroimage* **10**, 304–326 (1999).
5. M. Kohl, U. Lindauer, G. Royl, M. Kühl, L. Gold, A. Villringer, and U. Dirnagl, "Physical model for the spectroscopic analysis of cortical intrinsic optical signals," *Phys. Med. Biol.* **45**, 3749–3764 (2000).
6. D. A. Boas, T. Gaudette, G. Strangman, X. Cheng, J. J. A. Marota, and J. B. Mandeville, "The accuracy of near infrared spectroscopy and imaging during focal changes in cerebral hemodynamics," *Neuroimage,* **13**, 76–90 (2001).
7. M. Cope, "The development of a near infrared spectroscopy system and its application for non-invasive monitoring of cerebral blood and tissue oxygenation in the newborn infant," PHD thesis, University of London (1991).
8. J. Steinbrink, H. Wabnitz, H. Obrig, A. Villringer, and H. Rinneberg, "Determining changes in NIR absorption using a layered model of the human head," *Phys. Med. Biol.* **46**, 879–896 (2001).
9. M. Firbank, E. Okada, and D. T. Delpy, "A theoretical study of the signal contribution of regions of the adult head to near-infrared spectroscopy studies of visual evoked responses," *Neuroimage* **8**, 69–78 (1998).
10. M. Hiraoka, M. Firbank, M. Essenpreis, M. Cope, S. R. Arridge, P. van der Zee, and D. T. Delpy, "A Monte Carlo investigation of optical pathlength in inhomogeneous tissue and its application to near-infrared spectroscopy," *Phys. Med. Biol.* **38**, 1859–1876 (1993).
11. S. R. Arridge, M. Cope, and D. T. Delpy, "The theoretical basis for the determination of optical pathlengths in tissue: Temporal and frequency analysis," *Phys. Med. Biol.* **37**, 1531–1560 (1992).
12. M. Essenpreis, C. E. Elwell, M. Cope, P. van der Zee, S. R. Arridge, and D. T. Delpy, "Spectral dependence of temporal point spread functions in human tissues," *Appl. Opt.* **32**, 418–425 (1993).
13. P. van der Zee, S. R. Arridge, M. Cope, and D. T. Delpy, "The effect of optode positioning on optical pathlength in near infrared spectroscopy of brain," *Adv. Exp. Med. Biol.* **277**, 79–84 (1990).
14. S. J. Matcher, M. Cope, and D. T. Delpy, "*In vivo* measurements of the wavelength dependence of tissue-scattering coefficients between 760 and 900 nm measured with time resolved spectroscopy," *Appl. Opt.* **36**, 386–396 (1997).
15. G. M. Hale and M. R. Querry, "Optical constants of water in the 200 nm to μm wavelength region," *Appl. Opt.* **12**, 555–563 (1973).
16. S. Wray, M. Cope, D. T. Delpy, J. S. Wyatt, and E. O. Reynolds, "Characterization of the near infrared absorption spectra of cytochrome aa3 and haemoglobin for the non-invasive monitoring of cerebral oxygenation," *Biochim. Biophys. Acta* **933**, 184–192 (1988).
17. F. Bevilacqua, D. Piguet, P. Marquet, J. D. Gross, B. J. Tromberg, and C. Depeursinge, "*In vivo* determination of tissue optical properties: Applications to human brain," *Appl. Opt.* **38**, 4939–4950 (1999).
18. H. R. Heekeren, M. Kohl, H. Obrig, R. Wenzel, W. v. Pannwitz, S. Matcher, U. Dirnagl, C. E. Cooper, and A. Villringer, "Noninvasive

assessment of changes in cytochrome-c-oxidase oxidation in human subjects during visual stimulation," *J. Cereb. Blood Flow Metab.* **19**, 592–603 (1999).

19. M. Kohl, C. Nolte, H. R. Heekeren, S. Horst, U. Scholz, H. Obrig, and A. Villringer, "Changes in cytochrome-oxidase oxidation in the occipital cortex during visual stimulation: Improvement in sensitivity by the determination of the wavelength dependence of the differential pathlength factor," *Proc. SPIE* **3194**, 18–27 (1998).

20. R. Springett, J. Newman, M. Cope, and D. T. Delpy, "Oxygen dependency and precision of cytochrome oxidase signal from full spectral NIRS of the piglet brain," *Am. J. Physiol. Heart Circ. Physiol.* **279**, 2202–09 (2000).

21. V. Quaresima, R. Springett, M. Cope, J. T. Wyatt, D. T. Delpy, M. Ferrari, and C. E. Cooper, "Oxidation and reduction of cytochrome oxidase in the neonatal brain observed by in vivo near-infrared spectroscopy," *Biochim. Biophys. Acta* **1366**, 291–300 (1998).